Local Power Tally Bias and Error Autocorrelation from Exceeding Random-Number Stride in Monte Carlo–Fixed Source Simulation of Multiplying Medium

Arief Rahman Hakim[a], Douglas A. Fynan[a*]
[a]Department of Nuclear Engineering, Ulsan National Institute of Science & Technology,
UNIST-gil 50, Eonyang-eup, Ulju-gun Ulsan, 44919, Rep. of Korea
arief.rahman@unist.ac.kr, dfynan@unist.ac.kr
*Corresponding author

1. Introduction

At the heart of the Monte Carlo radiation transport method is the use of random numbers (RNs) to sample probability distributions. In practice, Monte Carlo codes use Pseudorandom Number Generator (PRNG) algorithms to generate sequence(s) of numbers whose sample statistics should approximate those expected from an unbiased random draw from a distribution, usually the uniform distribution on the interval [0,1]. During a simulation, each source particle starts its random walk from a predetermined position along the pseudorandom number sequence. The number of RNs skipped between each source particle is called the RN stride S. [1]

Some Monte Carlo code developers [2] appear to believe that Monte Carlo tallies are insensitive to the choice of stride including instances where the strides are exceeded by individual histories in the simulation based solely on the early study by Hendricks [1], despite a recent study [3] reporting factor of two magnitude errors in neutron flux tallies when the stride is exceeded. When history *i-1* exceeds the RN stride, the history will consume the adjacent RNs meaning history *i-1* is now correlated with history *i* (the exact same RNs generated by the PRNG are used in both histories). Hendricks and subsequently code developers argued that the same RNs consumed will be used for "*different sampling purposes*" in "*real problems*", so the correlation should be small/insignificant; however, a closer examination of the Monte Carlo sampling process in radiation transport problems readily reveals a finite and small number of actual processes (scattering polar and azimuthal angles, Russian roulette calls, reacting isotope nuclei, reaction rate channel, etc.) are sampled, and many real problems such are nuclear reactor cores consist of repeating lattices with similar material volumes in different spatial locations. Secondly, the two selected problems in [1] used to test the effects of stride exceedance are problematic because the first problem results—an oil-well logging neutron detection problem—suffered from high statistical uncertainties (5-10% relative standard deviations for flux tallies) easily masking stride-related simulation biases. The second problem, a 10% absorbing homogenous sphere, was ill-conceived because the problem symmetry and concentric flux tally surfaces suppress the effects of any particle track correlations.
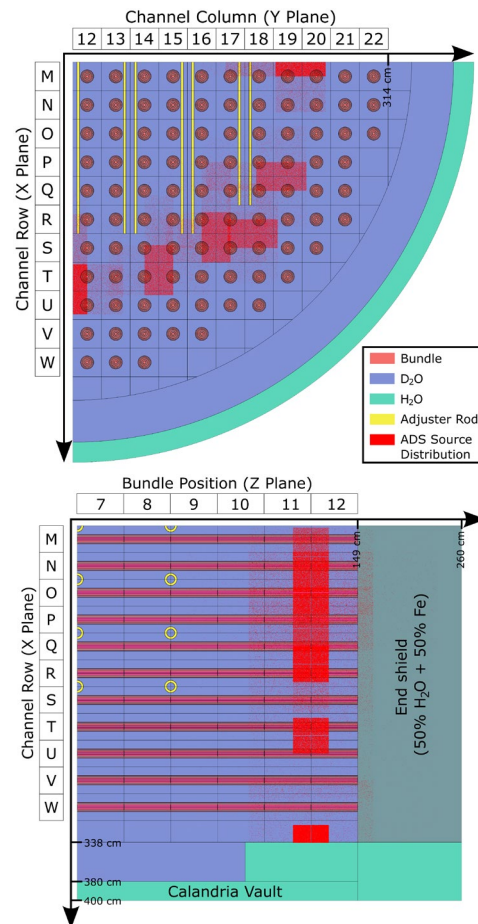

Figure 1. The cross-section view of the CANDU-6 model and sampled volumetric source.

This paper examines the effect of exceeding RN stride in Monte Carlo simulation of a subcritical, multiplying system motivated by our recent work simulating the ADS-CANDU concept [4], [5] summarized in Section 2. We observed all fixed-source neutron simulations of different subcritical states readily exceeded the code default RN stride up to a factor of 10^4. Section 3 presents the implementation of PRNG in Monte Carlo production codes and the mechanism of stride exceedance during the simulation of daughter particles produced from subcritical multiplication. Section 4 discusses the observed bias in the bundle-power tallies of the ADS-CANDU simulations indicated by both a statistically significant number relative errors exceeding two- and
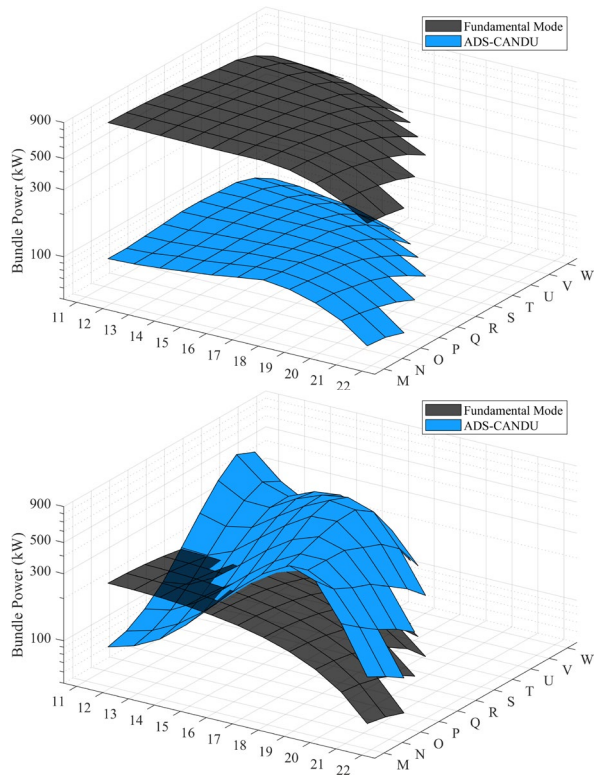
Figure 2. Bundle-power distribution at position 7 (upper panel) and 12 (lower panel) for 1288 MWe array-power (k_{eff} = 0.95009)
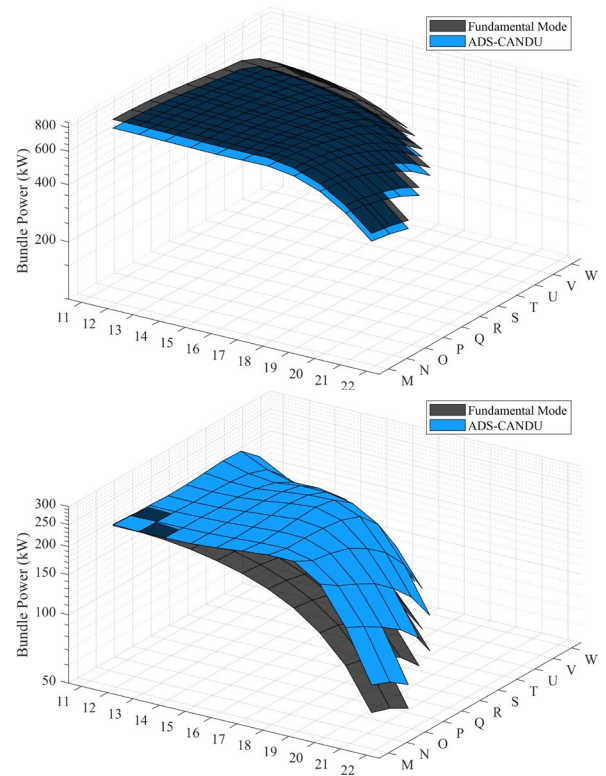

Figure 3. Bundle-power distribution at position 7 (upper panel) and 12 (lower panel) for 125 MWe array-power (k_{eff} = 0.99742)

three-sigma relative error bounds of an unbiased reference solution and strong autocorrelation of the relative errors correlated to the spatial relationship of bundle powers in the 3D core.

2. ADS-CANDU and 3D Bundle-Power Distribution

Previous study explores a new concept of steady-state power reactor operation from a subcritical CANDU-6 coupled to electron linear accelerators (eLINACs) configured between bundle-position 11 and 12 [4], [5]. The eLINACs produce hard bremsstrahlung which in-turn produce photoneutrons from the $D(\gamma,n)^1H$ reaction in the heavy water moderator, an accelerator-driven photoneutron source (ADS). Figure 1 shows the cross-section view of ADS-CANDU concept and sampled volumetric photoneutron-source in 1/8th model geometry [5] using the Monte Carlo code MCS [6].

The ADS acts as external neutron source to maintain the desired power level through a proportional relationship between the source strength and reactor subcriticality. For a subcritical reactor operating at steady-state (fission) power (P_f) driven by the external source, the fission neutron production rate (S_f) is related to the k_{eff} of the subcritical reactor and the source rate (S_{ADS}) according to the subcritical multiplication formula

$$S_f = \frac{S_{ADS}}{1 - k_{eff}}. \qquad (1)$$

Soluble boron is added to the moderator to artificially reduce the model's multiplication factor to match the desired k_{eff} during subcritical fixed-source neutron simulations.

Figures 2 and 3 show the reference power distribution for high-array (1288 MWe, k_{eff} = 0.95009) and intermediate-array (125 MWe, k_{eff} = 0.99742) powers compared to the fundamental mode (FM). The FM is the bundle power distribution obtained from criticality simulation of CANDU-6 reactor with the same MCS model using 120 inactive cycles, 500 active cycles, and 10 million histories per cycle. These simulation parameters ensure the FM is a reliable reference solution with all statistical variances of bundle powers less than 1% and fission source is believed to be fully converged with no numerical power tilts observed in [7].

Figure 2 establishes the high-array-power ADS capability to perturb the power distributions of large heavy water reactors. The induced fission chains are on average short (~20 generations predicted by Eq. 1) with most of the successive generations born locally near the ADS resulting in a distorted power distribution with power peaked towards the ADS locations, and the high-power bundle occurs at bundle position 11 and 12 (see lower panel of Fig. 2). In intermediate-array-power ADS, fission neutrons born in the vicinity of ADS arrays and successive generations are more likely to migrate and multiply towards the core center; however, the bundle-powers are still lower than the FM due to the

subcriticality of the system as seen in Fig. 3. For the purpose of discussion on stride exceedance in Section 4, readers should keep in mind that the high-power bundles are generally located in core center for intermediate-array-power case and vice versa for high-array-power case. The underlying physics of these source-driven problems with spatially coupled high and low power bundle positions make good test cases for particle track correlations when stride is exceeded.

3. PRNG Implementation in Monte Carlo Production Code

Linear Congruential Generator (LCG) is the predominant PRNG algorithm employed in Monte Carlo radiation transport codes. The general form of LCG is

$$\xi_{i+1} = (g\xi_i + c) \bmod M , \qquad (2)$$

for g, c, and M are selected integer constants (see the tabulated of recommended constants in [8]) and $\xi_{i=0,1,...,P}$ is the sequence of RN seeds where ξ_0 is the initial RN seed and ξ_P is the last seed before the pattern repeats defining the total length of the sequence called the period. To obtain RN distributed on U[0,1], the seed must be normalized with the base of the modulus M.
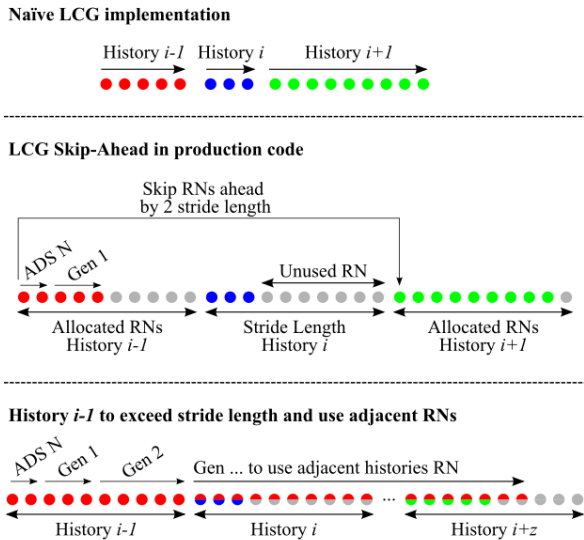

Figure 4. Naïve LCG (upper panel) and skip-ahead feature (middle panel) in Monte Carlo code.

The naïve LCG implementation is shown in Fig. 4 upper panel where Eq. (2) is evaluated sequentially as the random walk proceeds. After the particle history is terminated, the next source-particle history is initiated immediately with the proceeding RN seed in the sequence. However, this naïve approach is problematic for parallel simulation, so most production codes implement a feature to skip-ahead in the RN sequence by $(i \times S)$ steps further into the sequence. Now two subsets of RNs, $\xi_{iS<j\leq(i+1)S}$ and $\xi_{(i+1)S<l\leq(i+2)S}$, both from the same RN sequence can be generated independently on

other (different) processors quickly with algorithm presented in [9] allowing two histories to be simulated in parallel. When a particle is killed, the remaining RNs will not be generated or unused (see grey circles).

If a particle track is long which can occur in diffusing media, multiplying media, and variance reduction cases with particle splitting, the history may consume all of the allocated RNs. In this case, the LCG continues to march forward generating RNs from the next stride as illustrated in the lower panel of Fig. 4. Meanwhile a different processor is executing history i to which the second stride was allocated. Now particle histories $i-1$ and i are no longer independent because identical RNs are used in distribution sampling in both histories. If a particle track is very long and/or many daughter particles are simulated, the history may consume numerous successive strides.

4. Bundle-Power Bias and Spatial Autocorrelation from Exceeding RN Stride

4.1. Excessive Random Number Usage in Multiplying Medium

During the early study of ADS-CANDU concept [5], we discovered all of the fixed-source simulations exceeded the MCS default RN stride (S_{def} = 152,917 RNs) between three to six percent of the total histories. The RNs usage statistics for these simulations are summarized in Table I. These simulations were set aside and all cases were rerun using and extended stride (S_{ext}) with length greater than 10^{10} to ensure no history exceeded its allocated stride. In the heavy water reactor lattice under study, the average neutron undergoes several hundred thermal diffusion scattering collisions after slowing down in the optically thick moderator and before leaking back into the absorbing fuel bundles, so the RN use is amplified by several orders of magnitude relative to simulations of lattices with tight fuel pin pitch (e.g., fast reactors and light water reactor cores). The average RN use statistic is included in Table I for completeness noting that the RN usage distribution has a strong right-hand skew due to the presence of very long fission chains. Table I shows the deeply subcritical case for which Eq. (1) predicts short fission chains have some very long chains that exceed S_{def} and consumed ~135 adjacent strides causing significant bias in bundle power of up to 3.5%.

Table I. Random Number Usage Statistics for Subcritical ADS-CANDU Simulations

k_{eff}	RN use per history		Max. $\frac{\cdot}{S_{ext}}$	# history exceeding stride	$|\Delta P_b^{max}|$
	Average	Maximum			
0.95009	3.2E+04	1.9E+07	0.13%	3.7%	3.5%*
0.99742	4.4E+05	2.1E+09		5.9%	1.1%
0.99841	5.7E+05	2.1E+09	14%	6.0%	0.8%
0.99878	5.8E+05	2.1E+09		6.0%	1.2%
0.99908	6.2E+05	2.1E+09		6.0%	1.1%*

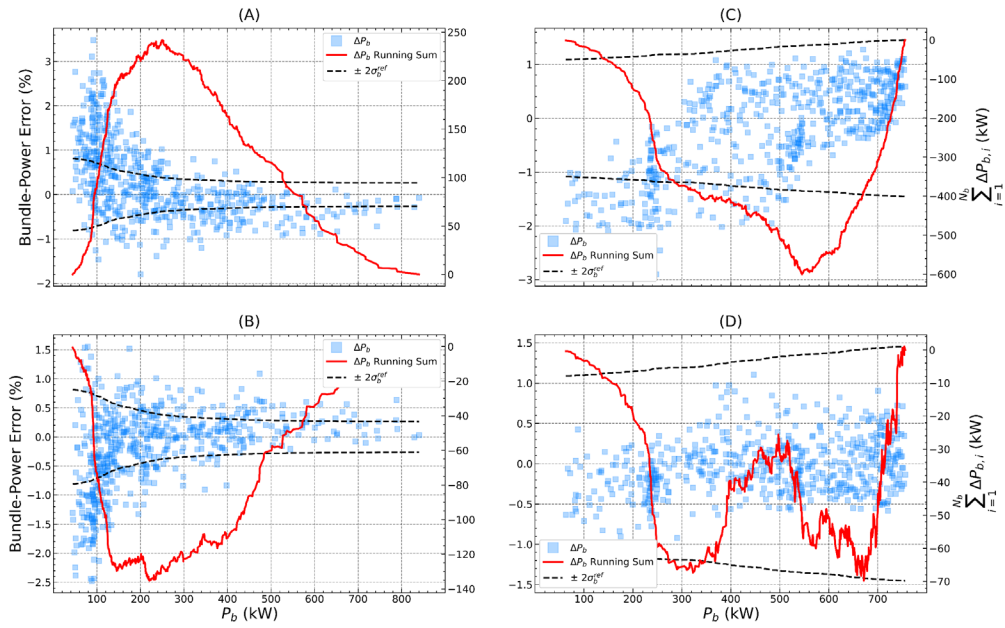*relative error exceeds $\pm 2\sigma_b$ confidence interval

Figure 5. Observed bundle-power errors of high-array-power (panels A and B) and intermediate-array-power (panels C and D) cases for $S = 152$. Each simulation is initialized with different RN seed.
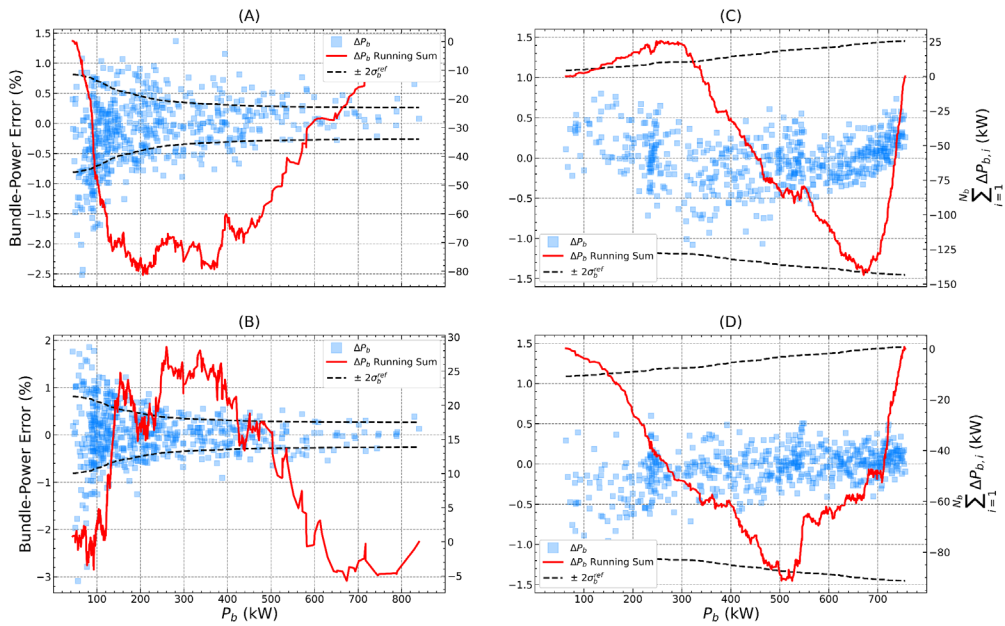

Figure 6. Observed bundle-power errors of high-array-power (panels A and B) and intermediate-array-power (panels C and D) cases for $S = S_{def}$. Each simulation is initialized with different RN seed.
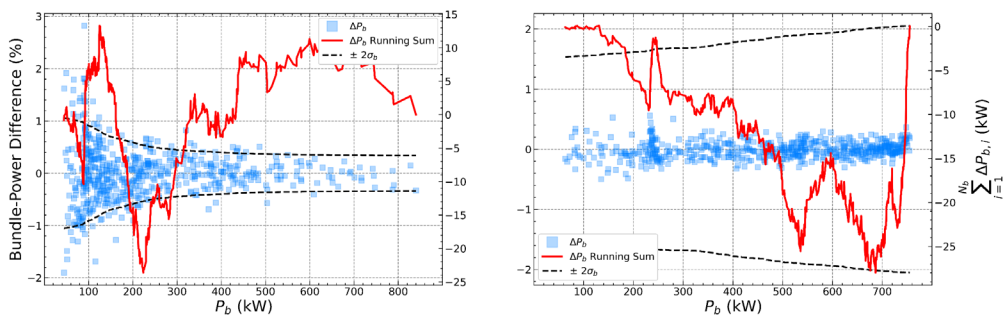

Figure 7. Bundle-power comparison from two independent reference runs of high-array-power (left panel) and intermediate-array-power (right panel) cases for $S = S_{ext}$. Each simulation is initialized with different RN seed.

The more serious situation is that all other simulations had a history with maximum RN usage a factor of 10^4 greater than the S_{def}, so that history consumed over 10,000 consecutive strides. If any of the 10,000 histories allocated to those strides were also long multiplication chains exceeding the stride, then there are groupings or layers of effective particle histories—source neutrons and successive fission neutrons produced—using the same *exact* RNs.

4.2. Spatial Autocorrelation of Bundle Power Errors

Preliminary comparison of element powers from the runs using the default stride to the extended stride revealed anomalies and statistically significant differences, so the high-array-power case (k_{eff} = 0.95009) and the fastest running intermediate-array-power case (k_{eff} = 0.99742) were selected for further investigation. For each subcritical case, multiple independent extended-stride runs initialized with a different RN seeds were simulated and tally statistics from multiple runs were merged [10] generating a clean reference dataset. Then two independent runs with reduced stride of 152 RNs guaranteeing more than 99% of histories exceed the stride were simulated for each subcritical state to augment the biased runs using the default stride.

Figures 5 and 6 compare the relative bundle-power errors of the reduced stride and default stride simulations to the respective reference runs using the extended stride. The left y-axes are the relative bundle power errors normalized by the reference bundle power, and the +/-2σ uncertainty bounds are MCS-calculated relative standard deviations from the merged reference simulations. The right hand-axes are running sums of the absolute bundle-power errors in ascending order from smallest powers to highest powers. The running sum starts and ends at zero because both simulations are scaled to the same core power of 2180 MWt.

The largest biases due to stride exceedance are observed for the short stride (152) deeply subcritical cases (Fig 5, panels A and B). Not only are there a statistically significant number of bundle power errors that exceed the +/-2σ and +/-3σ uncertainty intervals, 315 and 204 for Run A and 241 and 132 for Run B out of 570 total bundles, but also the signs of the errors show strong autocorrelation with spatial location in the core. The low-power bundles are located near the core center, and Run A low-power bundle powers are systematically overestimated and Run B bundles are systematically underestimated. Remembering that source neutrons are only generated at the core periphery, any neutron that reaches the center region is by de facto part of a long multiplication chain; we suspect particle tracks that use RNs from sequential strides are either preferentially propagated in the center region (Run A) or are diverged away from the center (Run B). The magnitudes of the maximum and minimum values of the running sum of errors, 242 kW and -135 kW, for 420 kW average bundle power are physically significant representing a spatial power tilt.

Run A of the near-critical case (panel C of Fig. 5) exhibits a severe power tilt exceeding the +/-2σ confidence interval of the reference case uncertainties with the power overestimated for the high-power bundles at the core center and underestimating power of the low-power bundles at the core periphery. Run B bundle powers are bounded by the confidence interval but autocorrelation of the error is still present. Not every stride exceedance case will show extreme bias because each case is still governed by stochastic processes, and biases of individual histories with opposite sign can cancel.

No strong argument using confidence interval analysis alone can be made about the bias present or not present in the default stride cases (Fig. 6) with 3-6% of histories exceeding the stride. Confidence interval statistics are 210 (37%) and 97 (17%) of bundle powers exceeding +/-2σ and +/-3σ uncertainty intervals for deeply subcritical Runs A and B, respectively. For near-critical Runs A and B, there are no bundles exceeding the confidence interval; However, the running sums clearly show autocorrelation of the errors although the magnitude of the accumulated errors are less than the reduced stride cases.

Figure 7 checks the expected behavior of the error scatter. In this comparison, the independent runs of the reference (extended stride) data sets were divided into two equal subsets and cross compared. The running sums are clearly consistent with the random behavior of errors expected from two independent runs with oscillations of the sum about the zero line and any accumulated error magnitude remaining small noting that the average bundle power is approximately 450 kW so the bundle standard deviations in absolute terms are approximately 5-10 kW. The ranking of bundles by power is somewhat arbitrary to allow for rough grouping by spatial location in the core, and when considering finite sample size, minor autocorrelations in regions of the independent variable range are likely to occur.

5. Conclusion

The study demonstrated that fixed-source simulations of multiplying medium can readily exceed the default random-number stride which is shown to induce significant bias in local tallies and strong autocorrelation of the relative errors. For the CANDU lattice studied, the error autocorrelation is related to the 3D spatial power distribution with biases manifesting as spatial power tilts. This is clearly contrary to the widely reported argument that Monte Carlo codes are insensitive to the stride exceedance [1], [2], [11]. We urge practitioners to monitor the random-number usage statistics for problems where excessive random-numbers use may occur (i.e. subcritical multiplication, highly diffusing media, aggressive particle splitting, etc.) and to re-investigate the impact of stride exceedance in production radiation

transport codes. Future study will characterize and quantify potential source of bias from correlated histories including critical review of legacy studies in [1]. In addition, it might be in interest to the nuclear community to identify which classes of radiation transport problems are susceptible to stride exceedance.

6. Acknowledgement

REFERENCES

[1] J. S. Hendricks, "Effects of changing the random number stride in Monte Carlo calculations," Nucl. Sci. Eng., vol. 109, no. 1, pp. 86–91, 1991, doi: 10.13182/NSE91-A23846.

[2] J. A.; Kulesza et al., "MCNP® Code Version 6.3.0 Theory & User Manual," vol. 28, 2022.

[3] E. Thomas and T. E. Booth, "Bad Estimates as a Function of Exceeding the MCNP Random Number Stride," 2014.

[4] D. A. Fynan, Y. Seo, G. Kim, S. Barros, and M. J. Kim, "Photoneutron production in heavy water reactor fuel lattice from accelerator-driven bremsstrahlung," Ann. Nucl. Energy, vol. 155, p. 108141, Jun. 2021, doi: 10.1016/j.anucene.2021.108141.

[5] A. R. Hakim and D. A. Fynan, "Flux Flattening Heavy Water Reactors with Accelerator-driven Photoneutron Source," Int. Conf. Phys. React. 2022 (PHYSOR 2022), pp. 3500–3509, 2022.

[6] H. Lee et al., "MCS – A Monte Carlo particle transport code for large-scale power reactor analysis," Ann. Nucl. Energy, vol. 139, p. 107276, 2020, doi: 10.1016/j.anucene.2019.107276.

[7] A. R. Hakim, Y. Seo, and D. A. Fynan, "Source Convergence in Monte-Carlo Criticality Simulation of CANDU-6 Reactor," Trans. Korean Nucl. Soc. Autumn Meet., 2022.

[8] P. L'Ecuyer, "Tables of linear congruential generators of different sizes and good lattice structure," Math. Comput., vol. 68, no. 225, pp. 249–260, 1999, doi: 10.1090/s0025-5718-99-00996-5.

[9] F. B. Brown, "Random Number Generation with Arbitrary Strides," American Nuclear Society Winter Meeting. 1994.

[10] F. B. Brown, "A Tutorial on Merging Tallies from Separate MCNP5 Runs," vol. 836, 2008.

[11] X-5 M. C. Team, "MCNP 5 Manual," 2003.